

## **SUPPLEMENTARY MATERIAL**

For the sake of replicability and completeness, additional methodological details and further analyses are included in this Supplementary material.

### **Inclusion/exclusion criteria**

Among all the subject under study, exclusion criteria were: (i) any neurological illness; (ii) history of cranial trauma with loss of consciousness longer than one minute; (iii) past or present substance abuse, except nicotine or caffeine; (iv) total intelligence quotient (IQ) smaller than 70; and (iv) for patients, any other psychiatric process, and (v) for controls, any current psychiatric or neurological diagnosis or treatment.

### **Preprocessing**

Signals were filtered between 1 and 70 Hz by means of a band-pass finite impulse response filter. A 50 Hz notch filter was also used to remove the power line artifact. Lastly, a three-steps artifact rejection algorithm was applied to minimize, mainly, electrooculographic and electromyographic contamination (1): (i) Independent Component Analysis (ICA) was carried out and, after visual inspection of a specialist, ICA components associated with artifacts were discarded (2); (ii) after ICA reconstruction, EEG data were divided into trials of 1 second length ranging from 300 ms before to 700 ms after stimulus onset, which ensures no overlapping with subsequent trials; and (iii) an automatic and adaptive trial rejection was performed by applying a statistical-based thresholding method.

### **Continuous wavelet transform and edge effects**

EEG recordings are non-stationary signals with changing properties over time. Wavelet transform takes into account these changes, providing an appropriate alternative to Fourier transform.

In this study, complex Morlet was used as mother wavelet. It provides a biologically plausible fit to EEG data (3). Complex Morlet wavelet is characterized by its localization

in time ( $\Delta t$ ) and frequency ( $\Delta f$ ). In this study,  $\Delta t$  and  $\Delta f$  were set to 1 to obtain a balanced relationship at low frequencies (1).

The coefficients of the continuous wavelet transform (CWT) are computed as the convolution between the EEG signal in each artifact-free trial,  $x(t)$ , and scaled and translated versions of the mother wavelet,  $\varphi(t)$ :

$$\text{CWT}(k, s) = \frac{1}{\sqrt{s}} \cdot \int_{-\infty}^{+\infty} x(t) \cdot \varphi^* \left( \frac{t-k}{s} \right) dt, \quad (1)$$

where  $s$  represents the dilation factor ( $s = \{s_i, i = 1, \dots, M\}$ ),  $k$  is the translation factor and the asterisk denotes the complex conjugation. The dilation factor was set to include frequencies from 1 Hz ( $s_1$ ) to 70 Hz ( $s_M$ ) in equally-spaced intervals of 0.5 Hz (1). Nevertheless, as we explained in the main text, only theta frequency band (4-8 Hz) was considered for the analyses.

EEG trials are finite and short-time recordings. Therefore, edge effects are not negligible (4). In this study, a cone of influence was defined in order to delimitate the time-frequency regions that included the biased wavelet coefficients (4).

## Brain network estimation

Connectivity matrices were obtained by means of phase-locking value (PLV). The PLV has become a useful tool to quantify the phase steadiness between pairs of electrodes (5), given its sensitivity to measure the neural synchronization, even between EEG oscillations with relatively small amplitude (6). As previously mentioned, this study was aimed at analyzing cognitive network dynamics. Thereby, the PLV was calculated in the theta frequency band (4-8 Hz).

Being able to use different approaches for computing the PLV, the CWT was used to extract the phase information from each trial (7). First, to calculate PLV between two signals, it is necessary to extract the instantaneous phase of each signal in a narrow bandwidth (8). CWT can be used to perform filtering and phase extraction in a single step (7). Thus, the instantaneous phases  $\varphi_x(k, s, \tau)$  and  $\varphi_y(k, s, \tau)$  of two EEG signals,  $x(t)$  and  $y(t)$ , can be used to define the phase differences as follows:

$$\Delta\varphi_{xy}(k, s, \tau) = \varphi_x(k, s, \tau) - \varphi_y(k, s, \tau), \quad (2)$$

where  $\tau$  represents each artifact-free trial.

Detailed procedures about the wavelet parameters and the minimization of the edge effects were reported in our previous studies (1, 9, 10).

PLV estimates the variability of the phase differences across successive trials, as follows:

$$PLV_{xy}(k, s) = w_{ij}(k, s) = \frac{1}{N_t} \left| \sum_{\tau=1}^{N_t} e^{(\Delta\varphi_{xy}(k, s, \tau))} \right|, \quad (3)$$

where  $N_t$  is the total number of artifact-free trials.

Functional connectivity matrices based on PLV were obtained by comparing the synchronization between all EEG channels. The values of the connectivity matrix ( $w_{ij}$ ) ranged between 0 and 1 (weighted network). A value of 1 was obtained with completely synchronized signals and a value of 0 implied an absence of synchronization. It means that no threshold was applied. This has the advantage that all the connections are considered (even the lower ones), but the computational cost increases comparing to a semi-weighted network.

## Network parameters

Networks can be described by several parameters. The present study was focused on five complementary features of the brain network: integration, segregation, connectivity strength, complexity and irregularity. The parameters that were used to quantify the previous network features are the following:

- The integration of the network was characterized by means of the characteristic path length. It is defined as the average shortest path length between all pairs of nodes in the network (11):

$$PL = \frac{1}{N} \sum_{i \in n} \frac{\sum_{j \in n, j \neq i} d_{ij}}{n-1}, \quad (4)$$

where  $d_{ij}$  indicates the minimum distance (i.e. the inverse of PLV) between electrodes  $i$  and  $j$ . Of note,  $N$  represents the number of nodes in the network ( $N = 29$ ).

- The segregation of the network was quantified by the averaged clustering coefficient (11). In the case of weighted networks, the averaged clustering coefficient can be generalized as follows to avoid the influence of the main connection weights:

$$CLC = \binom{N}{3} \sum_{i \in n} \sum_{j, h \in n} (w_{ij} w_{ih} w_{jh})^{1/3}, \quad (5)$$

where  $w_{ij}$  denotes the connection weight between electrodes  $i$  and  $j$ .

- The connectivity strength was computed using the network density as follows (10):

$$GD = \frac{\sum_{i=1}^N \sum_{j>i} w_{ij}}{T}, \quad (4)$$

where  $w_{ij}$  represents the connection weight between nodes  $i$  and  $j$ , and  $T = N(N-1)/2$  is the total number of connections in an undirected graph.

- The irregularity of the brain network was characterized by the Shannon Graph Entropy, defined in our previous work as follows (10):

$$H = \frac{-1}{\log_2 T} \sum_{i=1}^N \sum_{j>i} \frac{w_{ij}}{W} \log_2 \frac{w_{ij}}{W}, \quad (6)$$

where  $W$  is the sum of all weights of the graph and  $\log_2 T$  is a normalization factor introduced to ensure that  $0 \leq H \leq 1$ .

- The complexity of the brain network was estimated using the Shannon Graph Complexity, defined in our previous work as follows (10):

$$SGC = H \cdot \sqrt{\frac{1}{T-1}} \cdot \frac{\sigma}{\bar{w}}. \quad (7)$$

where  $\bar{w}$  is the average of all edge values of the graph and  $\sigma$  is the standard deviation of those values.

Importantly, Shannon Graph Entropy and Shannon Graph Complexity do not depend on the connectivity strength. Therefore, changes in these measures ensure that the network changes in the other parameters are not only due to changes in the connectivity strength.

## **Dynamical network modeling**

The steps of the proposed algorithm, individually adjusted for each subject, can be summarized as follows:

- 1) A specific connection (usually named as  $w_{ij}$  in graph theory context) of the pre-stimulus connectivity matrix is randomly selected.
- 2) The value of the connection,  $w_{ij}$ , is eventually modified with a probability  $P$ . Both the value of  $P$  and how it is modified depend on the specific model being considered, as we explain below.
- 3) The network features are computed for the modified connectivity matrix.
- 4) The MSE between the network parameters of the connectivity matrix in 3) and those of the connectivity matrix associated to the cognitive response is computed.
- 5) The steps 1), 2) 3) and 4) are repeated 5000 times and the MSE is stored for each iteration.
- 6) The connectivity matrix that minimizes the MSE is selected. The simulations showed that the MSE is a concave function with a minimum that varies for each subject. We checked that the minimum was always achieved before 5000 repetitions. Of note, the number of iterations required for reaching the minimum MSE is different for each subject.

The previous procedure was repeated six times (one for each model). The value of  $P$  and how it was modified depend on the model being considered as follows:

- i) Reinforcement of primary connections: The value of the connection randomly selected is increased a 1% with probability  $P = w_{ij}$  ( $w_{ij}$  ranges from 0 to 1).
- ii) Reinforcement of secondary connections: The value of the connection randomly selected is increased a 1% with probability  $P = 1 - w_{ij}$ .
- iii) Reinforcement of a connection at random. The value of the connection randomly selected is increased a 1% with probability  $P = 1$ .
- iv) Weakening of primary connections: The value of the connection randomly selected is decreased a 1% with probability  $P = w_{ij}$ .
- v) Weakening of secondary connections: The value of the connection randomly selected is decreased a 1% with probability  $P = 1 - w_{ij}$ .
- vi) Weakening of a connection at random. The value of the connection randomly selected is decreased a 1% with probability  $P = 1$ .

The percentage of change (1%) was heuristically determined as a compromise between goodness of fit and computational cost.

As previously mentioned, the dynamical cognitive network model randomly selected a node in each iteration. In order to minimize the possible bias due to the intrinsic stochastic behavior of the algorithm, all the experiment was repeated 100 times and MSE results were averaged across repetitions in each subject. Nevertheless, we observed that the variability among experiments for each subject was negligible.

## **Discarding confounding factors**

Studies of mental disorders through the EEG are prone to obtain inaccurate results due to the number of confounding factors. In order to avoid misinterpretation and prevent inappropriate conclusions, the influence of potential confounding factors on the clinical and network features was assessed. Thus, we found that the age and gender distributions, as well as the doses of the prescribed medication, did not produce a significant effect on

PLV values, network measures or cognitive data ( $p > 0.05$ ; Spearman's bivariate correlation test).

It must be noticed that all EEG measures are influenced by volume conduction. In order to minimize this effect, a well-known strategy is based on the assumption that volume conduction affects the connectivity estimates in a similar way in two different experimental contrasts (12). Spurious estimates can then effectively get rid by comparing both conditions (12). This is the approach followed in our study: comparing pre-stimulus and response during the cognitive task, both acquired during the performance of the oddball task, but in two different moments. In addition, short-scale synchronization is more influenced by volume conduction (5). However, we focused on theta band, which is associated with long-range interactions (13).

In order to discard possible influence of abnormal shape of the event-related potentials (ERPs), they are represented in the Figure 1S. In addition, P3b peak and latency for both groups are shown in the Table 1 of the main text. Finally, connectivity matrices are shown in the Figure 2S.

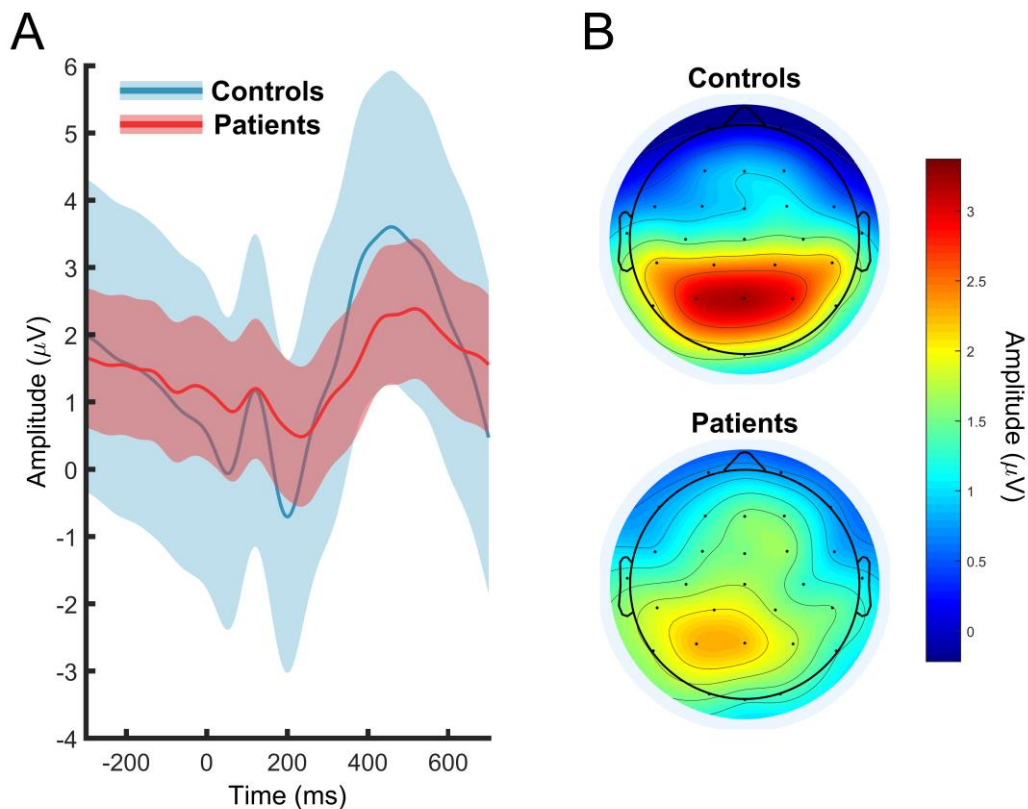


Figure 1S. (A) **P300 waveforms** at Pz electrode for controls (blue) and patients (red). (B) **Scalp maps depicting the P3b peak amplitude** (from 300 ms to 550 ms) for controls and patients.

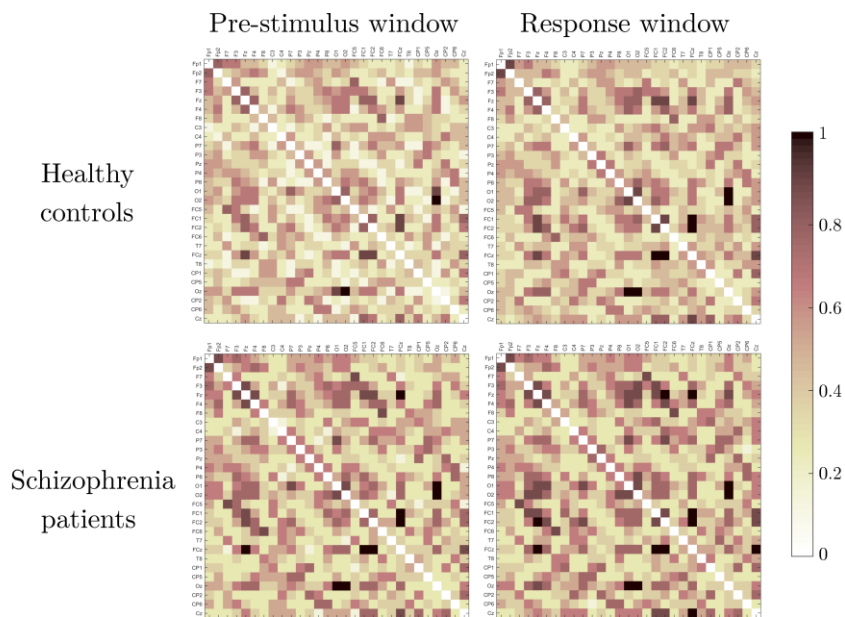


Figure 2S. **Averaged connectivity matrices.** The connectivity matrices are shown for controls and schizophrenia patients before (from -300 to 0 ms) and after (from 150 to 450 ms) stimulus onset.

### Weakening network models

Most of the subjects fitted a reinforcement model; however, in the case of 15% of the subjects (seven controls and six schizophrenia patients), a model based on weakening the connections was selected. For these thirteen subjects, Fig. 3S shows the distribution of the selected model for each group. Due to the low number of subjects, statistical analyses were not performed in this case.

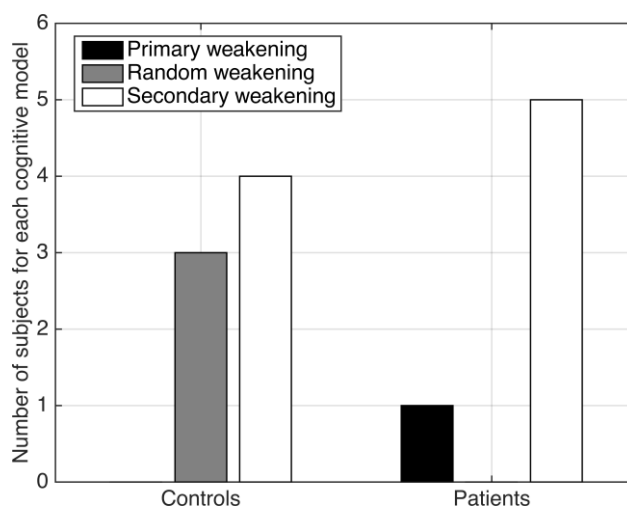


Figure 3S. **Histogram of the selected models and mean square error (MSE) distribution for each model.** Only the subjects that follow a model based on weakening the network connections were depicted in this histogram.

## **The relationship between cognition and network parameters**

Relationship between cognition and brain functioning was assessed by means of the correlations between results of the cognitive tests (z-scores corrected) and values of network measures (measured as the percent of change from pre-stimulus to cognitive response). For that purpose, Spearman's bivariate correlation test was used. Bonferroni correction was applied to correct for multiple testing ( $p$ -values were multiplied by 6 cognitive domains x 5 network parameters = 30). All the performed correlations are shown in Table 1S. Statistically significant correlations after Bonferroni correction ( $p < 0.05$ ) are highlighted in bold.

## **The relationship between cognition and symptoms**

Symptoms were assessed by means of the PANSS (z-scores corrected). Correlation between cognition and symptoms was studied by Spearman's bivariate correlation test. The performed correlations are shown in Table 2S. Statistically significant correlations ( $p < 0.01$ ) are highlighted in bold. The symptoms, summarized as the PANSS-total, are negatively correlated to verbal memory and processing speed (i.e., more symptoms are related to poorer cognitive performance).

These findings agree with the intuitive notion that more pronounced symptoms are usually linked to poorer cognitive performance (14). It was suggested that the negative and disorganized symptom dimensions are the reason for the strong correlation between symptoms and cognitive dysfunction in schizophrenia (14).

**Table 1S.** Correlation coefficient and  $p$ -values for all the possible comparisons between cognition and network parameters. Three correlations remain statistically significant after Bonferroni correction ( $p < 0.001$ , highlighted in bold).

		Integration	Segregation	Connectivity strength	Complexity	Irregularity
Verbal memory	$r$	-0.196	0.218	<b>0.423</b>	-0.190	0.169
	$p$ -value	0.042	0.027	<b>&lt;0.001</b>	0.048	0.070
Working memory	$r$	0.005	0.023	0.199	0.042	-0.034
	$p$ -value	0.484	0.422	0.040	0.357	0.383
Motor speed	$r$	0.044	-0.017	0.153	0.073	-0.062
	$p$ -value	0.352	0.442	0.090	0.264	0.296
Verbal fluently	$r$	-0.285	0.331	<b>0.499</b>	-0.160	0.159
	$p$ -value	0.007	0.002	<b>&lt;0.001</b>	0.087	0.087
Processing speed	$r$	-0.244	0.261	<b>0.472</b>	-0.178	0.166
	$p$ -value	0.016	0.010	<b>&lt;0.001</b>	0.060	0.073
Executive function	$r$	-0.029	-0.012	0.103	0.121	-0.137
	$p$ -value	0.402	0.459	0.186	0.147	0.118

**Table 2S.** Correlation coefficient and  $p$ -values for all the possible comparisons between cognition and symptoms. Two correlations are statistically significant ( $p < 0.01$ , highlighted in bold).

		Verbal memory	Working memory	Motor speed	Verbal fluently	Processing speed	Executive function
PANSS-positive	$r$	-0.177	-0.224	0.173	-0.106	-0.134	0.171
	$p$ -value	0.193	0.136	0.199	0.319	0.257	0.207
PANSS-negative	$r$	-0.282	-0.150	-0.035	-0.283	-0.354	0.033
	$p$ -value	0.081	0.233	0.433	0.101	0.038	0.439
PANSS-total	$r$	<b>-0.459</b>	-0.319	0.061	-0.281	<b>-0.478</b>	0.155
	$p$ -value	<b>&lt;0.01</b>	0.056	0.384	0.103	<b>&lt;0.01</b>	0.230

### The relationship between network parameters and symptoms

We also assessed the relationship between symptoms and network measures (as the percent of change from pre-stimulus to cognitive response) by Spearman's bivariate correlation test. The performed correlations are shown in Table 3S. Significant correlations ( $p < 0.01$ ) are highlighted in bold. The symptoms, summarized as the PANSS-total, are negatively correlated to segregation and irregularity, but positively correlated to complexity. On the other hand, positive symptoms, summarized as PANSS-positive, are negatively correlated to irregularity.

**Table 3S.** Correlation coefficient and  $p$ -values for all the possible comparisons between symptoms and network parameters. Four correlations are statistically significant ( $p < 0.01$ , highlighted in bold).

		Integration	Segregation	Connectivity strength	Complexity	Irregularity
PANSS-positive	$r$	0.153	-0.273	-0.314	0.413	<b>-0.434</b>
	$p$ -value	0.206	0.068	0.043	0.011	<b>&lt;0.01</b>
PANSS-negative	$r$	0.254	-0.331	-0.290	0.215	-0.178
	$p$ -value	0.084	0.035	0.057	0.123	0.170
PANSS-total	$r$	0.280	<b>-0.461</b>	-0.413	<b>0.465</b>	<b>-0.445</b>
	$p$ -value	0.064	<b>&lt;0.01</b>	0.010	<b>&lt;0.01</b>	<b>&lt;0.01</b>

### Topological network measures and cognitive variables: comparison with previous findings

Comparisons between network measures and cognitive variables are usually performed using a resting-state approach (15, 16) and sometimes during a cognitive task (17), but it is not usually assessed by analyzing the predisposition to change of the pre-stimulus activity. In our previous study (9), segregation was inversely associated with executive function and directly associated with working memory. Although, the same trend was found in this study, non-significant associations were found between such parameters after Bonferroni correction. This discrepancy can be easily explained due to the number of differences between both studies: (i) connectivity strength was not computed in the previous research; (ii) network parameters were computed using event-related coherence, which is not strictly a synchronization measure; and (iii) low-density EEG recordings were used (17 channels).

Despite the difficulty to compare the correlations observed in this study with previous findings, it seems natural that a direct correlation between global brain synchronization and cognitive performance exists. In fact, although Pachou *et al.* (2008) did not evaluate the change from pre-stimulus to cognitive response, they found a correlation in patients

between working memory load and global synchronization. This result could indicate that the cognitive effort required higher synchronization of the whole brain. The empirical evidence regarding the association between cognitive functions and network parameters was not so widespread some years ago (18). Nowadays, however, it is well-established that the architecture of functional brain networks is related to cognitive performance (19).

## References

1. Bachiller A, Poza J, Gómez C, Molina V, Suazo V, Hornero R (2015): A comparative study of event-related coupling patterns during an auditory oddball task in schizophrenia. *J Neural Eng.* 12: 16007.
2. Flexer A, Bauer H, Pripfl J, Dorffner G (2005): Using ICA for removal of ocular artifacts in EEG recorded from blind subjects. *Neural Networks.* 18: 998–1005.
3. Roach BJ, Mathalon DH (2008): Event-Related EEG Time-Frequency Analysis: An Overview of Measures and An Analysis of Early Gamma Band Phase Locking in Schizophrenia. *Schizophr Bull.* 34: 907–926.
4. Torrence C, Compo G (1998): A practical guide to wavelet analysis. *Bull Am Meteorol Soc.* 79: 61–78.
5. Lachaux JP, Rodriguez E, Martinerie J, Varela FJ (1999): Measuring phase synchrony in brain signals. *Hum Brain Mapp.* 8: 194–208.
6. Spencer KM, Nestor PG, Niznikiewicz MA, Salisbury DF, Shenton ME, McCarley RW (2003): Abnormal neural synchrony in schizophrenia. *J Neurosci.* 23: 7407–7411.
7. Bob P, Palus M, Susta M, Glaslova K (2008): EEG phase synchronization in patients with paranoid schizophrenia. *Neurosci Lett.* 447: 73–77.
8. Lachaux JP, Rodriguez E, Martinerie J, Varela FJ (1999): Measuring phase synchrony in brain signals. *Hum Brain Mapp.* 8: 194–208.
9. Gomez-Pilar J, Lubeiro A, Poza J, Hornero R, Ayuso M, Valcárcel C, *et al.* (2017): Functional EEG network analysis in schizophrenia: Evidence of larger segregation and deficit of modulation. *Prog Neuro-Psychopharmacology Biol Psychiatry.* 76: 116–123.
10. Gomez-Pilar J, Poza J, Bachiller A, Gómez C, Núñez P, Lubeiro A, *et al.* (2017): Quantification of graph complexity based on the edge weight distribution balance: Application to brain networks. *Int J Neural Syst.* S0129065717500320.
11. Rubinov M, Sporns O (2010): Complex network measures of brain connectivity: Uses and interpretations. *Neuroimage.* 52: 1059–1069.
12. Bastos AM, Schoffelen J-M (2015): A tutorial review of functional connectivity

- analysis methods and their interpretational pitfalls. *Front Syst Neurosci.* 9: 175.
13. Uhlhaas PJ, Roux F, Rodriguez E, Rotarska-Jagiela A, Singer W (2010): Neural synchrony and the development of cortical networks. *Trends Cogn Sci.* 14: 72–80.
  14. O’Leary DS, Flaum M, Kesler ML, Flashman LA, Arndt S, Andreasen NC (2000): Cognitive correlates of the negative, disorganized, and psychotic symptom dimensions of schizophrenia. *J Neuropsychiatry Clin Neurosci.* 12: 4–15.
  15. Micheloyannis S, Pachou E, Stam CJ, Vourkas M, Erimaki S, Tsirka V (2006): Using graph theoretical analysis of multi channel EEG to evaluate the neural efficiency hypothesis. *Neurosci Lett.* 402: 273–277.
  16. Smit DJ, Stam CJ, Posthuma D, Boomsma DI, de Geus EJC (2008): Heritability of “small-world” networks in the brain: A graph theoretical analysis of resting-state EEG functional connectivity. *Hum Brain Mapp.* 29: 1368–1378.
  17. Pachou E, Vourkas M, Simos P, Smit D, Stam CJ, Tsirka V, Micheloyannis S (2008): Working memory in schizophrenia: An EEG study using power spectrum and coherence analysis to estimate cortical activation and network behavior. *Brain Topogr.* 21: 128–137.
  18. Bullmore E, Sporns O (2009): Complex brain networks: graph theoretical analysis of structural and functional systems. *Nat Rev Neurosci.* 10: 186–198.
  19. Shine JM, Bissett PG, Bell PT, Koyejo O, Balsters JH, Gorgolewski KJ, *et al.* (2016): The dynamics of functional brain networks: integrated network states during cognitive task performance. *Neuron.* 92: 544–554.